




Research Article

One step sonochemical synthesis of single phase Sr-doped ZnO₂ nanorods



Deepesh Bhardwaj¹  · Dixit Prasher² · Anuj Dubey¹ · Vishal Dhiman² · Radha Tomar³

Received: 11 December 2020 / Accepted: 8 March 2021 / Published online: 29 March 2021

© The Author(s) 2021 

Abstract

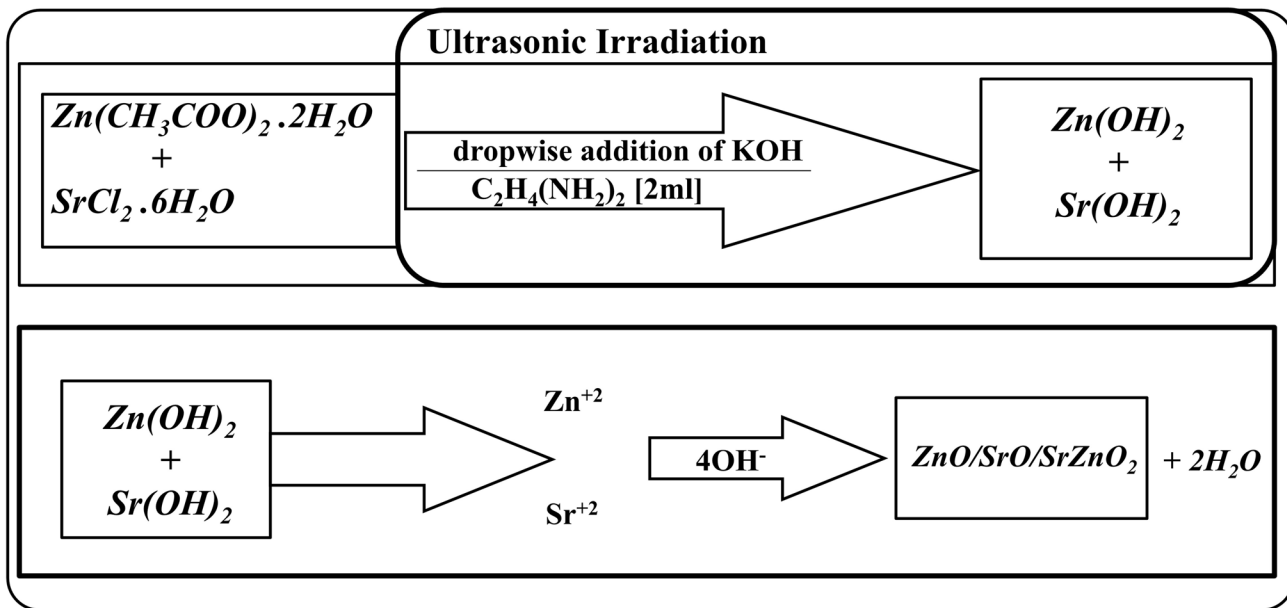
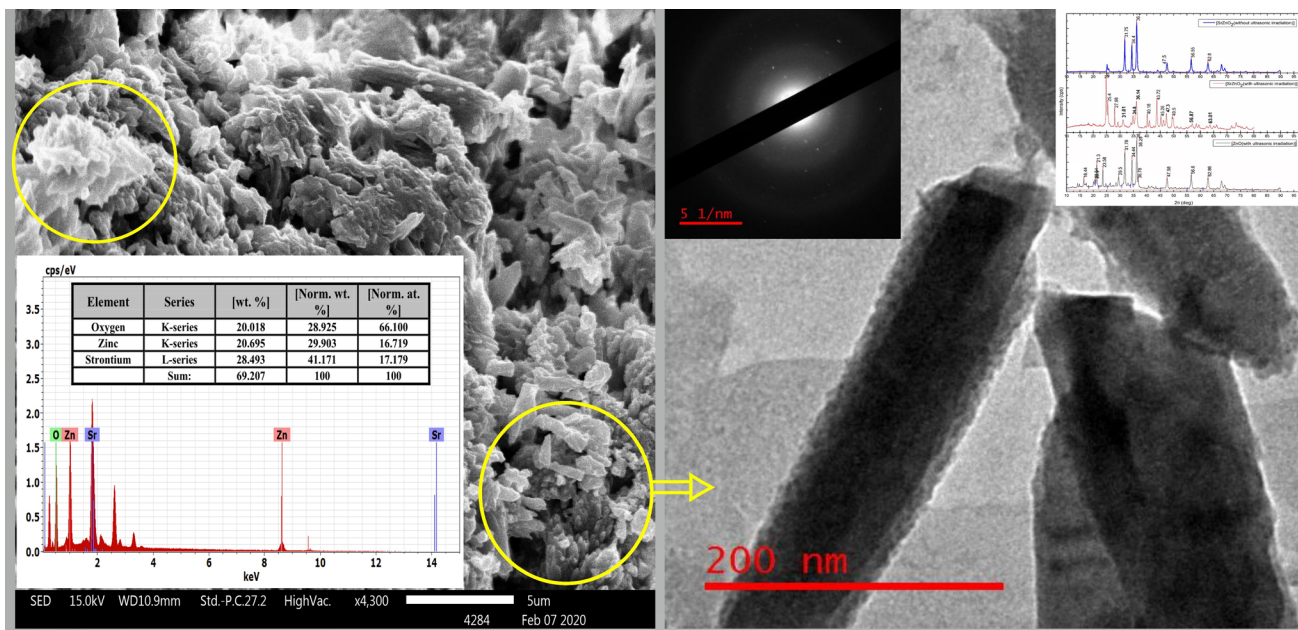
Single phase SrZnO₂ nanorods with average size of around 100 nm are synthesized by probe sonicator using ultrasonic waves at 60 W, 6 kHz for 3 h to observe the changes in optoelectronic properties of ZnO. The as grown SrZnO₂ has a single phase rod shaped structure. These nanorods were broadly characterized by different instrumental techniques like TEM, FESEM, EDAX, XRD, UV–Visible and FTIR for analysis of size, crystal structure, morphology and composition which acknowledge the formation of single phase crystalline ZnO and slightly amorphous SrZnO₂ nanorods. All these results suggest that single phase SrZnO₂ nano-composites can easily be synthesized by one step sono-chemical method.

✉ Deepesh Bhardwaj, bhardwajdeepesh@gmail.com | ¹Department of Chemistry, ITM Group of Institutions, Gwalior 474001, India. ²Department of Physics, Maharishi Markandeshwar (Deemed to be University), Mullana-Ambala, India. ³SOS Chemistry, Jiwaji University, Gwalior, India.



SN Applied Sciences (2021) 3:510 | <https://doi.org/10.1007/s42452-021-04479-7>

Graphic abstract



One step sonochemical synthesis of single phase Sr-doped ZnO₂ nanorods

Keywords Sonochemical synthesis · SrZnO₂ · ZnO · Nanorods · Optoelectronic property

1 Introduction

Recently, most of the research work on photo anodes has been focused on the nanostructures of TiO₂ [1]. However, the ZnO semiconductor could be a substitute for TiO₂

since, it has optoelectronics and luminescent pre-eminent properties with electronic affinity similar to that of TiO₂ [2]. ZnO has a comparable bandwidth gap of 3.37 eV, a high electronic mobility of 115–155 cm²V⁻¹ s⁻¹, high exciton binding energy of 60 eV and stability against photo corrosion [3]. Photovoltaic applications of ZnO and its nanocomposites are well studied but the applications of ZnO incorporated with different metal oxides are less explored in the field of photo catalysis and photoluminescence [4]. So far ZnO intrgrated with SrO are synthesized by hydrothermal, high energy ball milling, carbonate

decomposition, aerosol-assisted chemical vapour deposition (AACVD) [4] and combustion synthesis [7].

In recent time, ZnO coupled with SrO gained much attention as the photocatalyst and phosphore mainly due to its cost effectiveness. Moreover, the high band gap of SrO ($E_g = 5.5\text{--}5.9\text{ eV}$) with low conduction band in comparison of ZnO ($E_g = 3.37\text{ eV}$) also makes it a good choice. The position of valence band and conduction band of ZnO in ZnO/SrO heterojunction is between and above the valence band and conduction band of SrO respectively. This could help in improving the photo catalytic performance of these nanocomposites by hinder charge recombination to overcome with the problems like high energy and long reaction period as required by the methods [5] mentioned above. Herein, in this work we proposed a novel sonochemical synthesis of rod shaped SrZnO₂ nanocomposites in a 180 min. The as synthesized SrZnO₂ nanocomposites were characterized with different instrumental techniques to establish its crystal structure and surface properties. This is possibly the first report of sonochemical synthesis of single phase nanorods of SrZnO₂ as per best of the author's knowledge.

2 Experimental

2.1 Chemicals

Strontium chloride hexahydrate solution [SrCl₂·6H₂O], Zinc acetate dihydrate [Zn(CH₃COO)₂·2H₂O], Ethylenediamine [C₂H₈N₂], Potassium hydroxide [KOH] and double distilled (DD) water were used without any further purification.

2.2 Synthesis of rod shaped SrZnO₂

SrZnO₂ nanorods were synthesized using the ultrasonic irradiation via probe-sonicator taking Zn and Sr in 1:1 molar concentration. To obtain SrZnO₂, 0.1 M strontium

chloride hexahydrate solution (SrCl₂·6H₂O) was added to the 0.1 M [Zn(CH₃COO)₂·2H₂O] in 100 ml of distilled water. The resulting aqueous solution was stirred for 30 min before adding 2 ml of ethylene-di-amine as the capping agent. The solution was then sonicated for 3 h at 60 W, 6 kHz with the simultaneous addition of 50 ml 0.2 M potassium hydroxide (KOH) as a reducing agent. The Yellowish-white precipitate obtained was then washed 5–6 times with water-ethanol (3: 1) solution and dried for 8 h at 85 °C.

SrZnO₂ nanorods were also synthesized through wet chemical synthesis without using ultrasonic waves keeping all the concentrations of reagents same as used in sonochemical synthesis at 80 °C on hot plate magnetic stirrer. The as prepared sample is then dried at 80 °C in oven, washed with 25% ethanol and stored for characterization.

The ZnO without doping Sr is also synthesized using ultrasonic waves as mentioned above using 0.01 M ZnSO₄, 7.5% NH₃ and distilled water at 80 °C are used as precursors. The 0.01 M ZnSO₄ was mixed with 7.5% of NH₃ and taken in 100 ml burette. It was then drop wise added to a distilled water preheated at 80 °C and simultaneously sonicated for 3 h at 150 watt and 6kHz. The white ppt thus formed is washed with distilled water 6–7 times and dried in oven at 80 °C.

2.3 Mechanism of rod shaped SrZnO₂

Acoustic cavitation [6], formation of phase isolated micro-reactor [7] and the microsized droplets that confine chemical reactions within their interior are responsible for the formation of nanocomposites. These transient, localized hot spot with extremely high temperature and pressures are primarily responsible for chemical effects of ultrasound.

When 2 ml of ethylene-di-amine as the capping agent was added to a well stirred mixture of strontium chloride hexahydrate solution (SrCl₂·6H₂O) and zinc acetate [Zn(CH₃COO)₂·2H₂O]. The solution is then sonicated with dropwise addition of KOH as reducing agents, then zinc (Zn(OH)₂) and strontium hydroxide (Sr(OH)₂) are formed [8, 9]. When the sonochemical process continued, the Zn(OH)₂ and Sr(OH)₂ is separated into Zn²⁺ and Sr²⁺ ions and OH⁻ radical forming ZnO and SrO nuclei according to the last reaction as given in the Fig. 1. The dissolution–nucleation cycle, produces nanocomposites of SrZnO₂.

2.4 Characterization

To establish the Physiochemical structure of the synthesized material, different analytical techniques are used. X-ray diffraction (XRD) analysis is done using a fifth generation Rigaku (Modal no Mini Flex 600 XRD). Morphology and

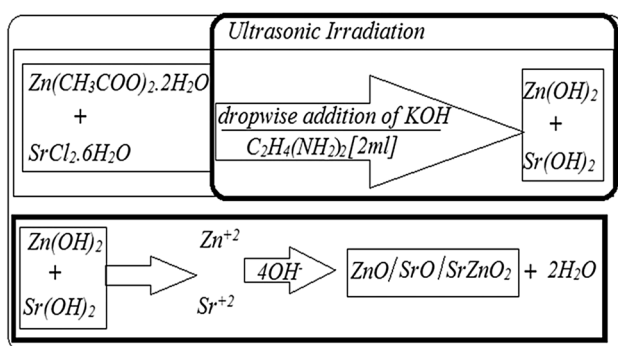


Fig. 1 Schematic representation of mechanism of synthesis

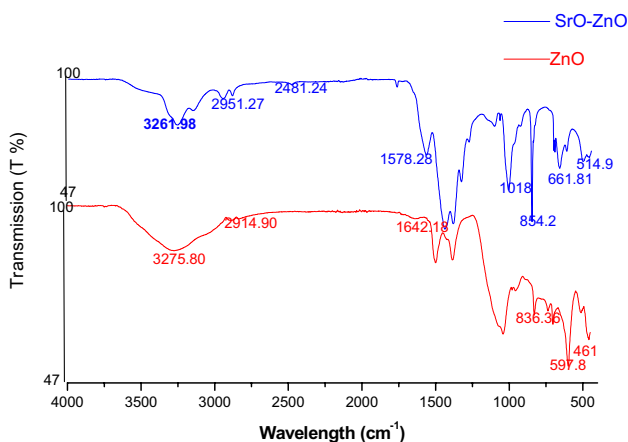


Fig. 2 FTIR spectra of ZnO and SrZnO₂

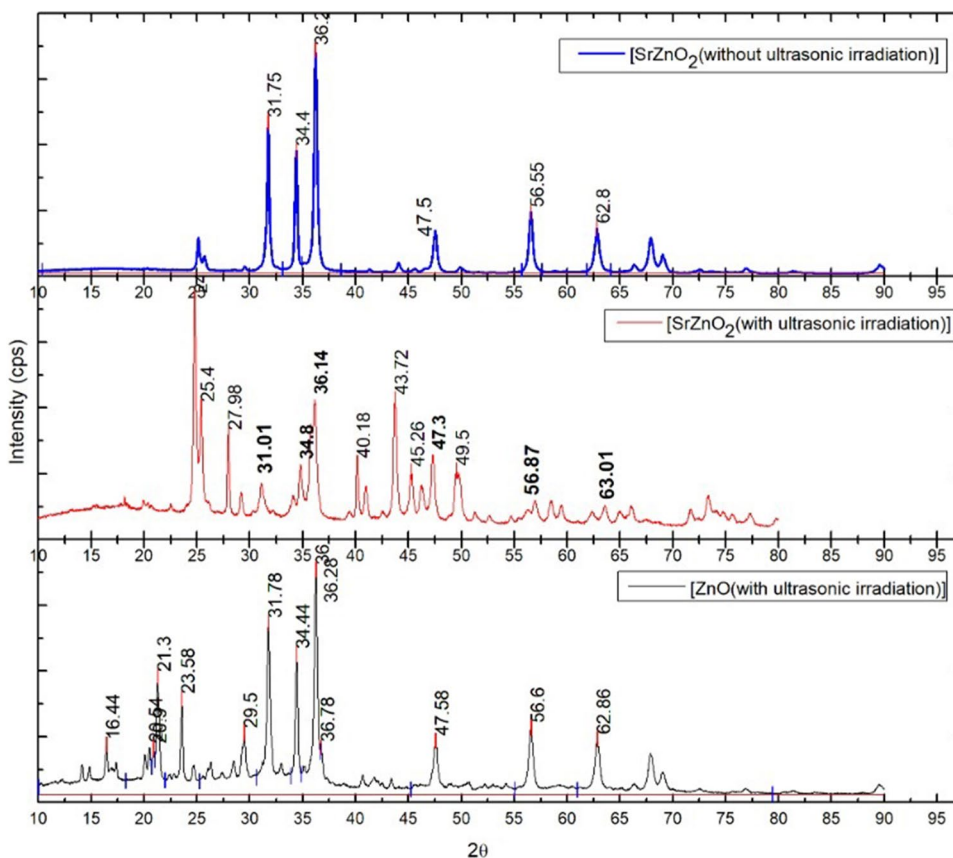
particle size of the composites are characterized by scanning electron microscopy (JEOLJSM6390LV). The chemical composition of synthesized material is also evaluated using Bruker Nano GmbH, Germany-EDAX. FTIR & UV-Vis spectroscopic techniques are also used to establish the synthesis of SrZnO₂ and change in energy bandgap.

3 Result and discussion

3.1 FT-IR analysis

FTIR analysis (Fig. 2) in a region between 4000 cm⁻¹ and 450 cm⁻¹ has been done to identify the synthesis of SrZnO₂. FTIR spectra give a wide and intense band between 550 cm⁻¹ and 450 cm⁻¹ [10] respectively for ZnO and SrO. Stretching mode of vibrations of the OH group of water molecules¹ can be attributed to the absorption peak at 3261 cm⁻¹. The presence of EDA in the SrZnO₂ nanostructures is confirmed by to the C–H elongation and flexion modalities attributed to the 3951 cm⁻¹ and 2914 cm⁻¹ respectively for SrZnO₂ and ZnO peaks. The band observed at 1578 cm⁻¹ and 1642 cm⁻¹ corresponds to the vibration C=O, due to the acetate group and zinc acetate used as one of the precursor. The peaks 1070–1012 cm⁻¹ are due to stretching vibration SrO. The band observed at 854 cm⁻¹ is attributed to the vibration of anti symmetric stretching of SrO. It is important to take into account that the SrO species affects the spectra and it is observed that the displacement in the ZnO band at 514 and 461 cm⁻¹ attached to the ZnO peaks which is assigned as a mode of elongation of Sr–O which is due to the Sr⁺² present in the composite

Fig. 3 X-ray diffractogram of ZnO and SrZnO₂ sono-chemically synthesized and SrZnO₂ without sonochemical synthesis



sample of SrZnO_2 . These results confirm the presence of SrO and ZnO in the composition [11].

3.2 XRD analysis

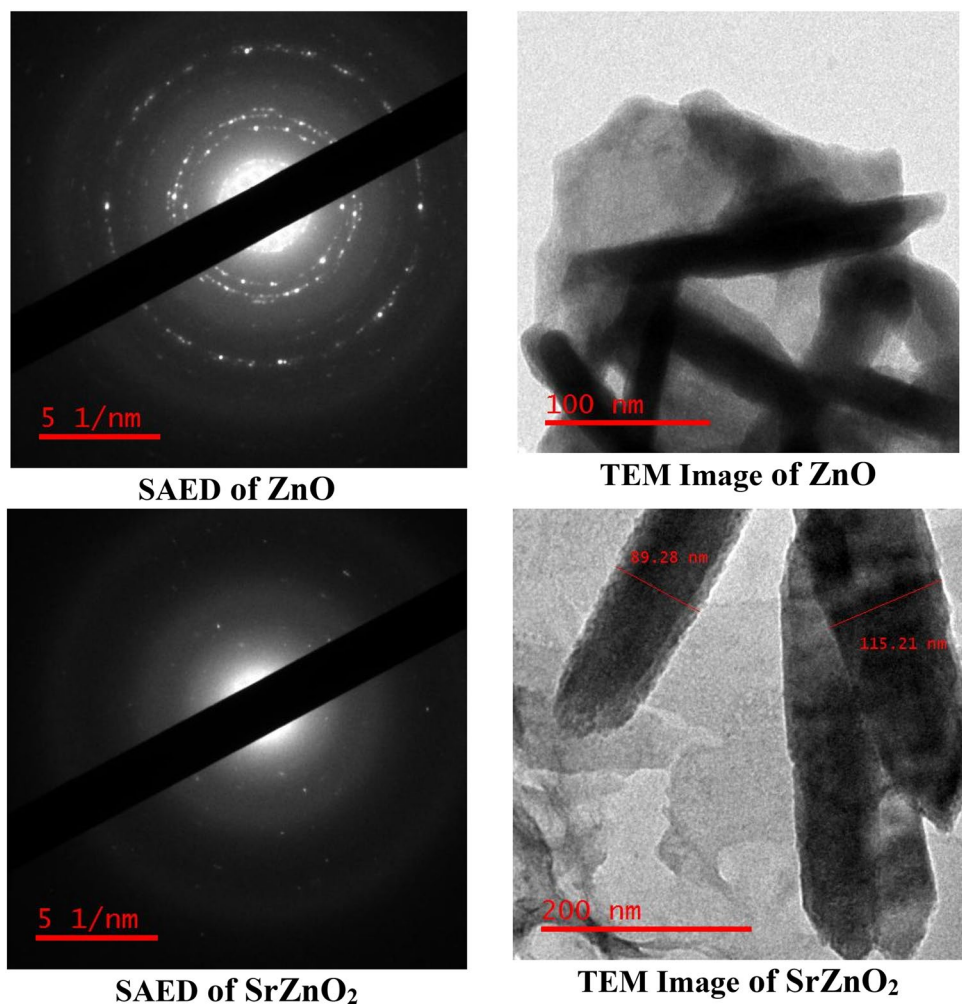
Figure 3 shows the X-ray diffraction pattern of SrZnO_2 and ZnO synthesized sonochemically and synthesis of SrZnO_2 without ultrasonic irradiation. Orientations (100), (002), (101), (102), (110), (103) and (112) of different intensities can be identified as the hexagonal structure (wurtzite) of ZnO according to JCPDS sheet 036–1451. The dimensional effect of strontium ($R_{\text{Sr}}/R_{\text{Zn}}$ ratio=1.96), is probably the origin of the formation of different nanocrystalline phases of ZnO [12]. The peak at 36.2° (JCPDS card no 800075) is assigned particular for ZnO in case of all the three materials [13]. The new Peaks observed at 2θ close to 31.75 (100), 34.4 (002), 47.5 (102), 56.55 (110) and 62.8 (103) in both with and without ultrasonic synthesis of SrZnO_2 indicates the presence of SrO in the composition. (JCPDS no. 0060520) [14]. The difference in atomic size causes changes in defect density, induces stress, network

distortion and leads to a reduction in oxygen supply. The reticular constants calculated from the most important peaks and the relation of the relative intensities $I(191)/I(109)$ in the diffraction model of the ZnO and SrZnO_2 at room temperature, respectively.

3.3 TEM analysis

TEM images (Fig. 4) of the ZnO nanoparticles and SrZnO_2 shows rod shape structures with an average particle size of approx 100 nm. The corresponding SAED images are indicating the crystalline nature of the nanocomposites of ZnO and less crystalline SrZnO_2 . The width of ZnO and SrZnO_2 nano rods are approximately 89 nm. Results obtained by the TEM are in agreements with the results of XRD. The selected area electron diffraction (SAED) pattern shows distinct bright rings in case of pure ZnO which confirms the preferential orientation of nanocrystals and crystallinity whereas in case of SrZnO_2 it indicates the less crystalline with rod shaped structures. The two sets of visible six-fold symmetrical and concentric diffraction spots

Fig. 4 SAED and TEM images of ZnO and SrZnO_2



in the SAED pattern of ZnO correspond to its hexagonal shape [13]

3.4 SEM and EDAX analysis

Typical SEM micrograph (Fig. 5) of the SrZnO₂ nanoparticles shows that the shapes of nanocomposites are close to rod shaped. The flower like shapes of hexagonal rods of ZnO is also confirmed from the previous work of the author [8]. It is expected that the initially form flower like structures can split into its hexagonal rods during sonochemical synthesis.

EDAX (Energy-dispersive X-ray spectroscopy) spectrum (Fig. 6) shows four peaks which were identified as atom % of oxygen (66.1%), zinc (16.7%) and strontium (17.1%) (Fig. 6). This percentage of oxygen, zinc and strontium is in agreement of the formation of SrZnO₂ nanocomposites.

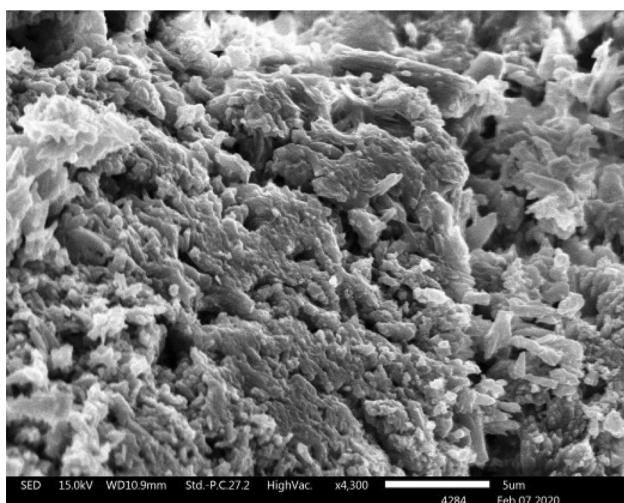


Figure 5. SEM images of SrZnO₂

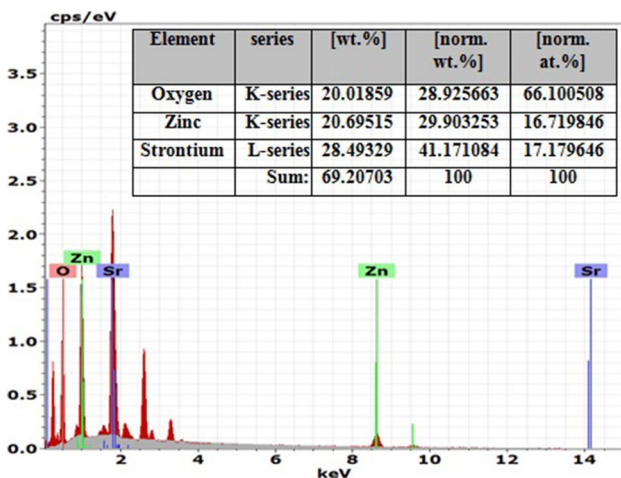


Fig. 6 EDAX results of SrZnO₂

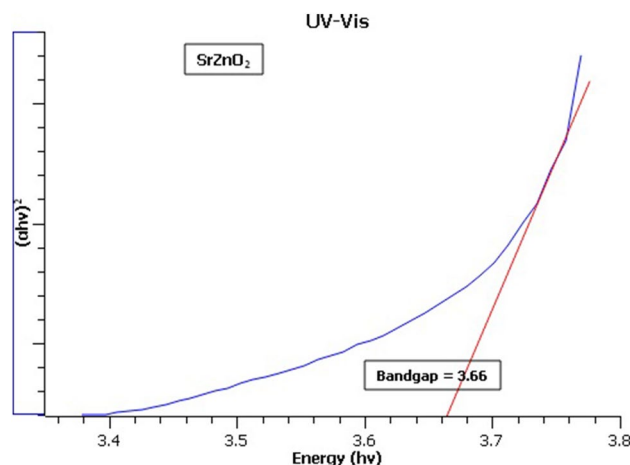


Fig. 7 UV-Vis results of SrZnO₂

3.5 UV-Vis analysis

Figure 7 shows the UV optical studies of SrZnO₂ composites. Optical studies confirm that the bandgap of SrZnO₂ nano composites clearly shifts to higher value as compare to pure ZnO from 3.31 [15] to 3.66. This increase in bandgap is due to the decrease in lattice spacing because of assimilation of Sr into ZnO lattice. Bandgap value can also be affected by factors like impurity, lattice distortion, and strain [16].

4 Conclusion

It is clearly established from this work that Sr integrated ZnO nanorods were synthesized by a simple, low-cost, ultrasonic method. Structural characterization revealed the incorporation of Sr⁺² into the ZnO network. This is the first report of SrZnO₂ nanorods by sonochemical method as per the best knowledge of authors. The inclusion of strontium in ZnO and formation of SrZnO₂ is increased to 3.66 from 3.31 of pure ZnO.

Acknowledgement Authors are grateful to Madhya Pradesh Council for Science Technology, Bhopal, MP, India for providing necessary financial support (File no 3134/CST/R & D/Phy & Engg. and Pharmacy/2018/05.02.2019) for this work and Dr. A.P.J Abdul Kalam Central Instrumentation Facility, Jiwaji University for providing valuable instrumentation facilities.

Declarations

Conflict of interest The authors declare that they have no conflict of interest

Open Access This article is licensed under a Creative Commons Attribution 4.0 International License, which permits use, sharing, adaptation, distribution and reproduction in any medium or format, as

long as you give appropriate credit to the original author(s) and the source, provide a link to the Creative Commons licence, and indicate if changes were made. The images or other third party material in this article are included in the article's Creative Commons licence, unless indicated otherwise in a credit line to the material. If material is not included in the article's Creative Commons licence and your intended use is not permitted by statutory regulation or exceeds the permitted use, you will need to obtain permission directly from the copyright holder. To view a copy of this licence, visit <http://creativecommons.org/licenses/by/4.0/>.

References

1. Wan T, Ramakrishna S, Liu Y (2018) Recent progress in electrospinning TiO₂ nanostructured photo-anode of dye-sensitized solar cells. *J Appl Polym Sci* 135(1):45649. <https://doi.org/10.1002/app.45649>
2. Greene LE, Yuhas BD, Law M, Zitoun D, Yang P (2006) Solution-Grown Zinc Oxide Nanowires. *Inorg chem* 45(19):7535–7543. <https://doi.org/10.1021/ic0601900>
3. Lee CP, Li CT, Fan MS, Li SR, Huang YJ, Chang LY, Ho KC (2016) Microemulsion-assisted zinc oxide synthesis: morphology control and its applications in photoanodes of dye-sensitized solar cells. *Electrochim Acta* 210:483–491. <https://doi.org/10.1016/j.electacta.2016.05.174>
4. Shukla A, Kaushik VK, Prasher D (2014) Growth and characterization of Mg_xZn_{1-x}O thin films by aerosol-assisted chemical vapor deposition (AACVD). *Electron Mater* 43:61–65. <https://doi.org/10.1007/s13391-013-3039-9>
5. Taikar DR, Joshi CP, Moharil SV, Muthal PL, Dhopte SM (2010) Synthesis and luminescence of SrZnO₂ phosphors. *J Lumin* 130(10):1690–1693. <https://doi.org/10.1016/j.jlumin.2010.03.033>
6. Bang JH, Suslick KS (2010) Applications of ultrasound to the synthesis of nanostructured materials. *Adv Mater* 22(10):1039–1059. <https://doi.org/10.1002/adma.200904093>
7. Hinman JJ, Suslick KS (2017) Nanostructured materials synthesis using ultrasound. *Top Curr Chem (Z)* 375(12):1–36. <https://doi.org/10.1007/s41061-016-0100-9>
8. Bhardwaj D, Sharma P, Khare PS (2013) Synthesis of whorl shaped zinc oxide nanostructure crystals by simple wet synthesis route. *Mater Lett* 111:134–136. <https://doi.org/10.1016/j.matlet.2013.08.090>
9. Askarinejad Azadeh, Alavi Mohammad Amin Morsali, Ali (2011) Sonochemically Assisted Synthesis of ZnO Nanoparticles: A Novel Direct Method. *Iran J Chem Chem. Eng.* 30(3):75–81. http://www.ijcce.ac.ir/m/article_6236_55545624fd235c982cb7c8356731abe4.pdf
10. Kleinwechter H, Janzen C, Knipping J, Wiggers H, Roth P (2002) Formation and properties of ZnO nano-particles from gas phase synthesis processes. *J Mater Sci* 37(20):4349–4360. <https://doi.org/10.1023/A:1020656620050>
11. Babu KS, Reddy AR, Sujatha C, Reddy KV (2013) Mallika AN (2013) synthesis and optical characterization of porous ZnO. *J Adv Ceram* 2:260–265. <https://doi.org/10.1007/s40145-013-0069-6>
12. Yang Z, Sun L, Ke C, Chen X, Zhu W, Tan O (2009) Growth and structure properties of La^{1-x}Sr_xMnO_{3-σ} (x= 0.2, 0.3, 0.45) thin film grown on SrTiO₃ (001) single-crystal substrate by laser molecular beam epitaxy. *J Cryst Growth* 311(12):3289–3294. <https://doi.org/10.1016/j.jcrysgro.2009.03.039>
13. Chou HS, Yang KD, Xiao SH, Patil RA, Lai CC, Vincent Yeh WC, Ho CH, Liouc Y, Ma YR (2019) Temperature-dependent ultraviolet photoluminescence in hierarchical Zn. ZnO and ZnO/Zn nanostructures *Nanoscale* 11:13385. <https://doi.org/10.1039/c9nr05235frsc.li/nanoscale>
14. Kumar B, Kumar S, Singh V, Vohra A, Chauhan N, Goyal R (2020) Preparation of strontium doped mesoporous ZnO nanoparticles to investigate their dye degradation efficiency. *Nano Express* 1(3):030015. <https://doi.org/10.1088/2632-959X/abc393>
15. Harish S, Sabarinathan M, Archana J, Navaneethan M, Nisha KD, Ponnusamy S, Hayakawa Y (2017) Synthesis of ZnO/SrO nanocomposites for enhanced photo catalytic activity under visible light irradiation. *Appl Surf Sci* 418:147–155. <https://doi.org/10.1016/j.apsusc.2017.01.164>
16. Basu S, Rana B, Barman A, Chatterjee S, Jha SN, Bhattacharyya D, Sahoo NK, Anup KG, Shiv K (2014) Structural, optical and magnetic properties of sol-gel derived ZnO: Co diluted magnetic semiconductor nanocrystals: an EXAFS study. *J Mater Chem C* 2:481–495. <https://doi.org/10.1039/C3TC31834F>

Publisher's Note Springer Nature remains neutral with regard to jurisdictional claims in published maps and institutional affiliations.